Journal of Hydrology, 78 (1985) 1—17
Elsevier Science Publishers B.V., Amsterdam — Printed in The Netherlands

[5]

CALIBRATION OF A MASS TRANSPORT MODEL USING ENVIRONMENTAL TRITIUM

J.C. HERWEIJER, G.A. VAN LUIJN and C.A.J. APPELO*

Instituut voor Aardwetenschappen, Vrije Universiteit, 1081 HV Amsterdam (The Netherlands)

(Received October 31, 1984; revised and accepted December 6, 1984)

ABSTRACT

Herweijer, J.C., Van Luijn, G.A. and Appelo, C.A.J., 1985. Calibration of a mass transport model using environmental tritium. J. Hydrol., 78: 1—17.

Tritium profiles of groundwater were obtained by detailed vertical sampling of a 20-m thick aquifer comprising fluvioglacial sediments in the central part of The Netherlands. Using the known environmental tritium input time series since 1951, these profiles were used to calibrate the Random Walk model of T.A. Prickett et al. To perform this procedure the model was modified to allow vertical use and a time-dependent non-instantaneous input of a decaying radioactive tracer.

During this calibration the following parameters were varied: (1) geological geometry (position and extent of a clay lens); (2) permeability variations; (3) ratio of net precipitation and effective porosity; and (4) longitudinal and transverse dispersivity. The calibrated model was hence used to predict the flushing of manure contamination from the aquifer.

The applied calibration technique has proved useful to test and roughly calibrate the hydraulic properties estimated from the logs of a limited number of borings, with the accuracy needed for mass-transport modelling. Compared with the very detailed drilling program that is usually required to obtain such detailed information, this tritium-based calibration seems competitive for shallow phreatic aquifers.

1. INTRODUCTION

In the northwest Veluwe (central Netherlands) serious groundwater contamination occurs due to heavy manure disposal on agricultural land. In a study of nitrate contamination of the main aquifer in this area, Appelo et al. (1983) showed the usefulness of detailed sampling at a 1-m interval for obtaining hydrochemical profiles of the aquifer. Tritium analyses of these samples were found enlightening in showing anomalous groundwater flow due to heterogeneities within the aquifer.

* To whom all correspondence should be addressed.

0022-1694/85/$03.30

The purpose of the present study is to show that hydrochemical profiles can also be analysed using an advection—dispersion mass-transport model. Such an analysis normally requires a very detailed knowledge of aquifer properties, since flowpaths have to be modelled closely. It will be shown, that modelling of tritium as an environmental tracer can give additional information for an accurate description of mass transport. As such, this study relates to similar work in which tritium (resulting from thermo-nuclear bomb testing in the atmosphere) is used as a hydrological tracer (Carlston et al., 1960; Egboka et al., 1983). As far as we know, environmental tritium has not been used till now to calibrate both the variations of hydraulic properties and the geometric configuration of heterogeneities with the accuracy needed for mass-transport modelling.

The Random Walk model, developed by Prickett et al. (1981), was modified and used to calculate mass transport in a cross-section parallel to the horizontal flow direction. Modifications were also made to allow the time-dependent input of a decaying radioactive tracer (tritium) to be modelled.

The modified model was extensively tested for its proper functioning. A sensitivity analysis of the advection parameters (geometry of an internal clay layer, permeability, porosity) and the dispersion coefficients was made using the tritium data. With the "best-fit" of this analysis nitrate transport was modelled, to find the vertical distribution and residence time of nitrate in the aquifer.

2. GENERAL DESCRIPTION OF THE STUDIED AREA

The Hierdensche Beek valley is a lowland area with both natural terrain and cultivated areas. For the present study a part of the valley was selected in which both types of land use occur, with contrasting qualities of infiltrated water and consequently of groundwater. Fig. 1 shows the distribution of land use. Detailed lithological descriptions and depths of piezometers were available from nine existing observation wells. Electrical resistivity soundings were made to further delineate the extent of the aquifer. Five additional borings were carefully (without water injection) bailed and equipped with three piezometers at different depths in the aquifer. To obtain detailed vertical samples, miniscreens were taped at desired depths on the outer side of the piezometer tube before its installation. The miniscreens are connected to the surface by 4-mm I.D. polyethylene tubings; water samples are obtained by applying vacuum suction to the tube ends at the surface.

2.1. Geological setting

The Hierdensche Beek valley is a sedimentary basin located between two ice-pushed ridges of unconsolidated Pleistocene fluvial sands (Fig. 2). It is

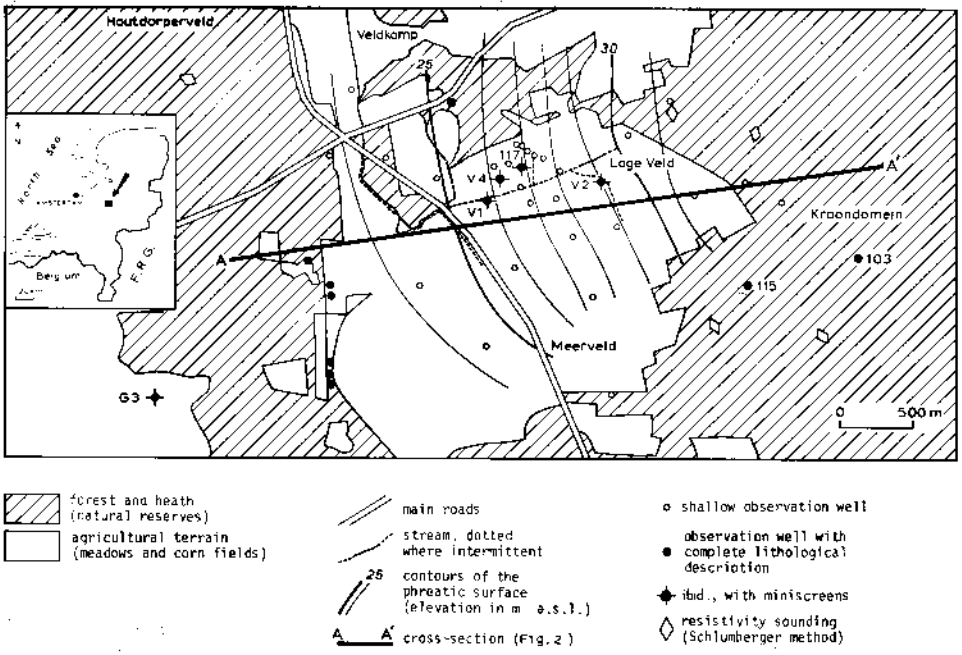

Fig. 1. The investigated area (land use, monitoring network and contours of the phreatic water table).

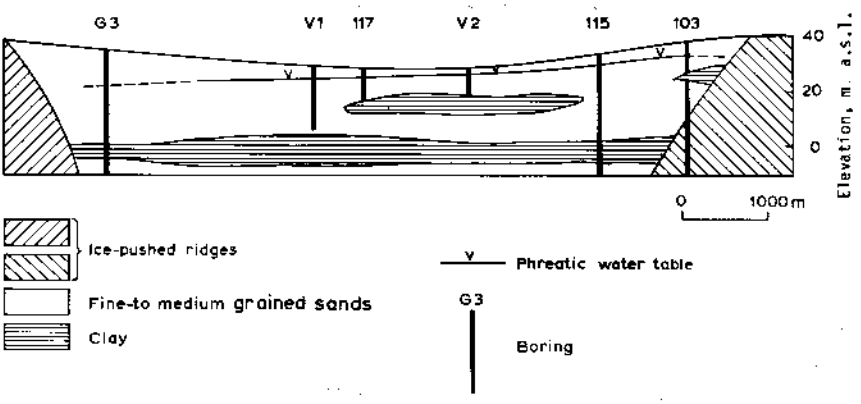

Fig. 2. Cross-section A—A' (for location see Fig. 1).

drained towards the north by a small brook, the Hierdensche Beek. During the Saalian glacial period the basin was filled with the Drenthe formation consisting of sediments partly eroded from the ice-pushed ridges, partly supplied by melt water of the ice-mass which was situated just north of the

basin (Crommelin and Maarleveld, 1952). During periods when the basin was closed by the ice-mass, clayey/loamy sediments were deposited (lymnoglacial). The intermediate periods can be characterised by deposition of poorly sorted coarse to very coarse sediments supplied by small channels descending from the ice-pushed ridges. A clay layer at approximately mean sea level (m.s.l.) extends under the whole area between the ice-pushed ridges; it serves as an aquiclude. Another, less extensive and discontinuous clay zone is present at 18—20 m above m.s.l. and several small clay lenses occur along the flank of the buried ice-pushed ridge at the east. The principal aquitard of this type will be referred to as "clay lens".

2.2. Hydrological conditions

Fig. 1 shows that the direction of groundwater flow is towards the west and the southwest. At the western and southwestern boundaries the phreatic surface forms a continuum with the piezometric surface of the underlying aquifer and the phreatic surface of the ice-pushed ridge aquifer. At the eastern boundary the difference between the phreatic surface of the shallow aquifer and that of the ice-pushed ridge aquifer is ~ 10 m. It is assumed that the local clay lenses and the erosional surface between the ice-pushed ridge and the basin fill cause a discontinuity in the phreatic surface. The base of the aquifer is the continuous clay layer at m.s.l. All wells in the area that penetrate layers below this clay layer show a piezometric level that is several metres below the phreatic surface.

The hydraulic gradient of the shallow aquifer varies from 0.003 to 0.005. The average annual recharge of the shallow aquifer is estimated at 365 mm (Meinardi, 1974). The whole area functions as a recharge area and only during a short period of the year is precipitation directly discharged by the drains. During six months of the year a very small base flow occurs in the brook (Hierdensche Beek); flow measurements indicate that this can be neglected in comparison with the amount of water that infiltrates and flows through the aquifer to the western boundary.

The saturated aquifer thickness varies from 20 m in the west to 27 m in the east. Permeability values have only been estimated from grain-size analysis (Boonstra and De Ridder, 1981). Fig. 3 shows the permeability variations of some layers within the aquifer. Due to the heterogeneous (fluvioglacial) depositional environment lateral correlation is impossible. This low degree of layer correlation makes it reasonable to assume that the average permeability is lower than the arithmetic means. The effective porosity is evaluated from the grain-size data with formulae given by Kovács (1981), indicating values of 25—30%. These are considered an overestimation, since the formulae were developed for well-sorted sands and a low degree of sorting in general tends to diminish porosity.

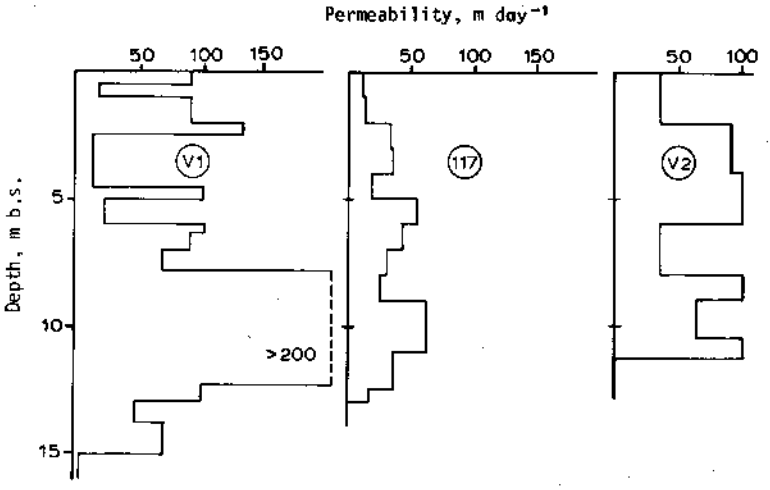

Fig. 3. Results of permeability analysis (from grain-size analysis) for different layers within borings V*1*, *117* and V*2*.

2.3. Hydrochemical and tritium data

Fig. 4 shows the results of miniscreen water sample analyses plotted as Vasak diagrams (Vasak et al., 1981).

The upper part of these diagrams shows a NO_3^-—Cl^-—K^+—Ca^{2+} water type of low pH (4—5) which is typical for infiltrated manure-contaminated water. Nitrate concentrations are up to four times the World Health Organization standard for drinking water of 50 mg l^{-1}.

The vertical variation of ion concentration can result from either areal variation of infiltration water quality or from chemical interaction with aquifer sediments (e.g., adsorption or redox processes). Nitrate is absent at depths of more than 8 m below the surface in borings V*1* and *117*. Fe and Mn concentrations increase simultaneously with the disappearance of NO_3^-, which indicates that reduction (denitrification) can be the cause of the absence of NO_3^-. Nitrate concentrations also diminish in the lower part of boring V2, but here Fe and Mn are absent. In the lower part of this boring there is also a decrease of Cl^- and SO_4^{2-} concentrations, which suggests a dilution with water infiltrated in the heath area upstream. Groundwater infiltrated in the heath area has a very low ion content which is essentially equal to the content in precipitation multiplied by a concentration factor due to evapotranspiration.

In the denitrifying zone of borings V*1* and *117*, HCO_3^- should replace NO_3^- in the water according to the reaction:

$$4NO_3^- + 5CH_2O \rightarrow 2N_2 + 4HCO_3^- + CO_2 + H_2O \qquad (1)$$

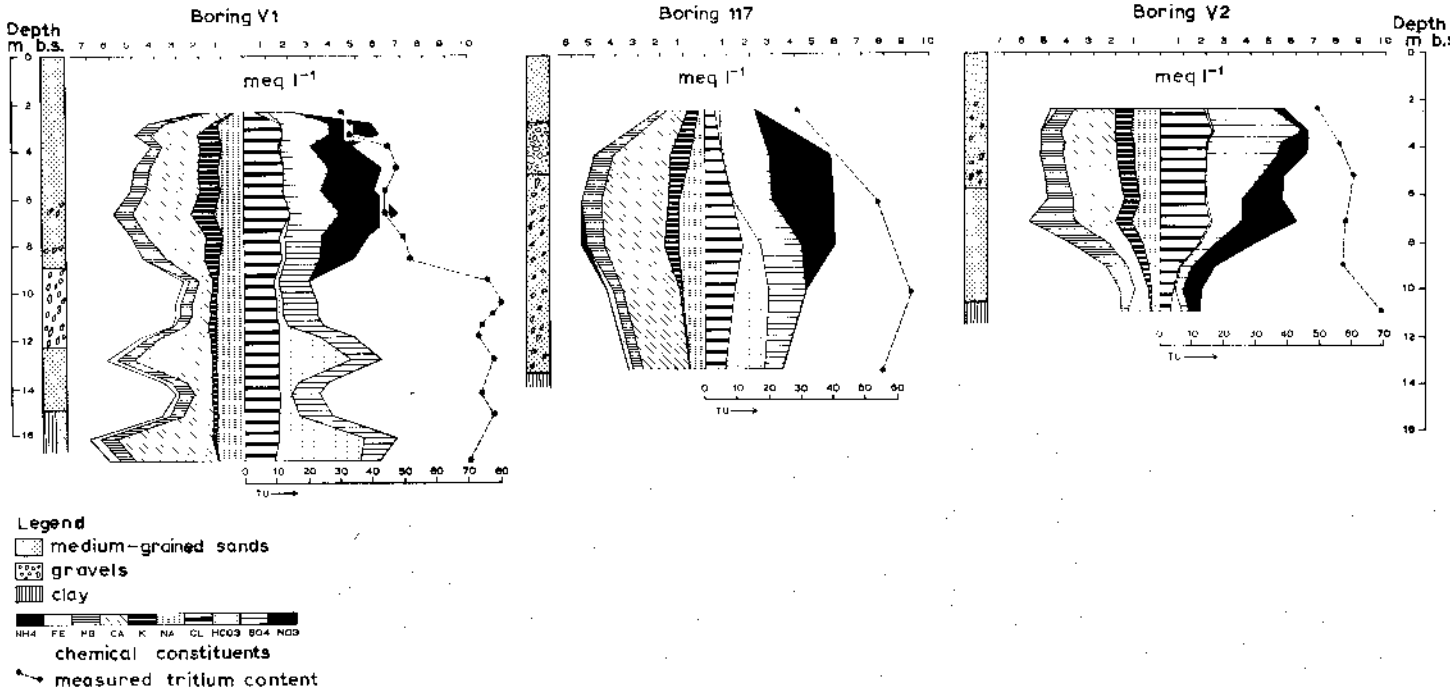

Fig. 4. Vasak diagrams of borings V*1*, *117* and V*2*.

90 %

Clearly from Fig. 4, however, the amount of HCO_3^- in the lower part of the borings is less than the NO_3^- concentration in the upper part. The water is undersaturated with respect to calcite, with exception of the two lowermost samples in boring V*1* which are from a low-permeability zone that extends down to the aquiclude. The lower HCO_3 concentration can therefore not result from precipitation of calcite.

Two explanations can be offered for the relatively low HCO_3^- concentration. The first is that NO_3^- concentrations are lower in the infiltration areas related with this depth and that no mixing by dispersion occurs between the water qualities created in the different infiltration areas. It is surprising, however, that Cl^- and SO_4^{2-} are uniform with depth, and show no decrease in concentration at the depths where total ion content decreases. This decrease would be expected since Cl^-, SO_4^{2-} and NO_3^- concentrations are often correlated in groundwater which shows pollution by manure disposal.

Another more attractive explanation involves cation exchange with the aquifer sediments. The water in the upper zone which still contains NO_3^-, has a low pH and Al concentrations of 0.3 mmoles l^{-1}, so that the exchange complex of the aquifer material is in part occupied by Al^{3+} ions. Denitrification raises pH so that Al in solution precipitates as $Al(OH)_3$; consequently, Al from the exchange complex goes into solution, to be exchanged for Ca^{2+}. This reaction can be schematized by:

$$2Al^{3+} - X + 3Ca^{2+} + 6HCO_3^- \rightarrow 3Ca^{2+} - X + 2Al(OH)_3 + 6CO_2$$

where X represents the exchange complex.

The reaction is thus triggered by the pH increase which follows the denitrification, but of course depends on the presence of an exchange complex. The increase of HCO_3^- and Ca^{2+} in water at 12 m below the surface in boring V*1* is then explained by the very coarse-grained nature of the sediment, with an inherently low cation exchange capacity.

Tritium profiles in the borings show no distinct peak, except boring V*1* which shows a marked contrast at 8 m below the surface.

3. THE RANDOM WALK MODEL

The Random Walk model was designed to solve the advection–dispersion equation which describes mass transport by flowing groundwater (e.g., Bear, 1972). It is based on a finite-difference technique which calculates piezometric heads and flow velocities for each nodal point. An interpolation scheme ensures a detailed velocity field between these nodal points.

Particles representing the contaminant are generated and traced by the model, the advective displacement of a particle being calculated by multiplying the local velocity with the time step. For both longitudinal and

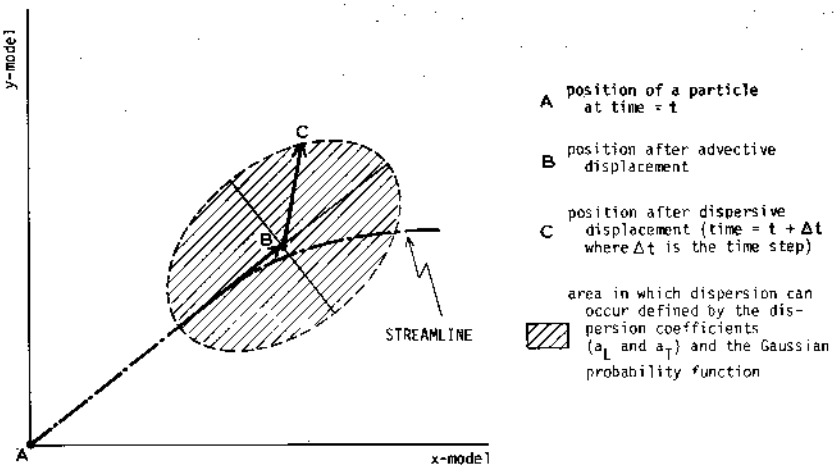

Fig. 5. Flow concept used in the Random Walk model (modified after Prickett et al., 1981).

transverse dispersive displacement, the absolute value of maximum displacement depends on the velocity and the dispersion coefficients. The actual dispersive displacement is calculated by multiplying the maximum displacement with a random number. For the longitudinal component this results in a forward or backward movement along the stream line and for the transverse component in a movement perpendicular to the streamline to the left or to the right (Fig. 5).

After each time step the coordinates of all particles are stored. At any desired time the number of particles in each cell can be counted and calculated as the contaminant concentration at each nodal point.

3.1. Adjustment of the model

Every two-dimensional groundwater model can in principle be used to analyse one-dimensional flow through a vertical section of an aquifer. It requires the following adjustments (Fig. 6):

(1) Assume a confined aquifer whose thickness is one length unit. This implies that transmissivity in fact represents permeability.

(2) Use for each cell along the side of the model, which in the adjusted version corresponds to the topographical surface, an injection well to simulate the aquifer recharge. The injection rate is then defined as:

$$Q = P_{eff} \cdot (\text{length})$$

where P_{eff} = effective precipitation; and length = cell-length along topographical surface.

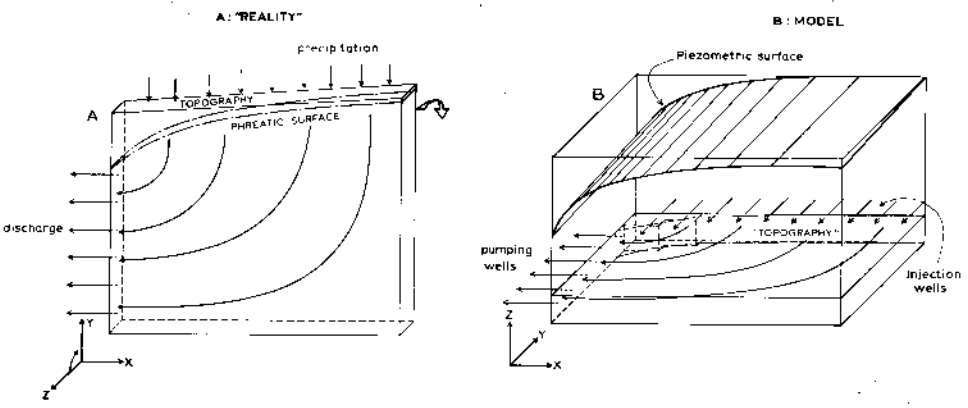

Fig. 6. Three-dimensional diagram showing the cross-sectional groundwater model.

(3) If the decline in phreatic level along the flow direction reduces the saturated thickness appreciably, this should be taken care of by adjusting the discretisation of space (Fig. 6B).

To check the proper functioning of the adjusted model, an aquifer with a constant saturated thickness and permeability was modelled. For this case simple analytical solutions are available (Ernst, 1973). First, modelled heads were compared with analytically calculated heads. With a 21 x 15 node model the error was less than 1% for each node. Secondly, for three particles launched at different positions, infiltration depths and travel times were compared with analytical calculations (Fig. 7). For the 21 x 15 grid the error in all cases is less than 2%.

When the model was tested several difficulties were encountered, caused mainly by the no-flow cells designed at essential places in the model (to match the topographical surface, or to simulate an internal clay lense). It was, for example, necessary to change the velocity interpolation scheme around the no-flow cells. This was done in the same way as shown by Prickett et al. (1981) for the edges of the original model.

Another difficulty was that the original model did not account for different permeabilities when calculating the random (dispersive) component. This automatically leads to an incorrect enrichment of particles in the cells where flow is restricted (by a relatively low or zero permeability). The nearly zero flow rate which appears here reduces the calculated dispersion value to zero and hence the possibility for the particle to leave the cell. When a particle was brought into such a no-flow cell, representing clay layers, the solution finally adopted was to put the particle back to its position before dispersive displacement and calculate a new random displacement. This was repeated as many times as necessary until the particle entered a zone of unrestricted flow.

$$d = \frac{x}{x+x_i} D$$

$$t = \frac{nD}{N} \ln\left(\frac{D}{D-d}\right)$$

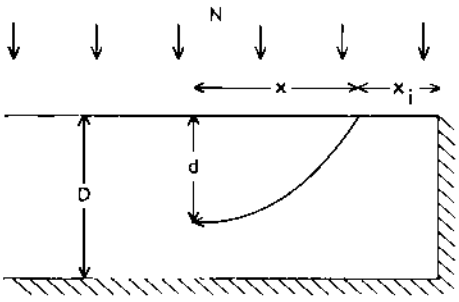

Fig. 7. Analytical solutions for flow in a cross-section of a homogeneous aquifer (d = infiltration depth; t = travel time; after Ernst, 1973).

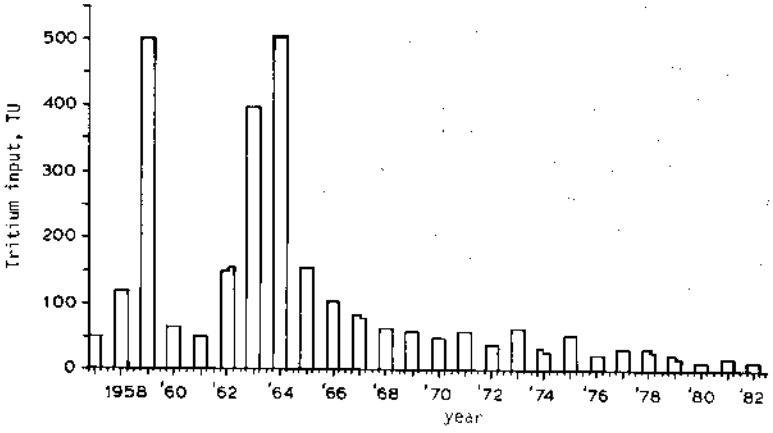

Fig. 8. Tritium time series from 1957 (modified after Appelo et al., 1983).

3.2. Modelling tritium decay

Fig. 8 shows the tritium time series used as model input. It was assumed that input occurred only during recharge periods (October—March). To incorporate tritium decay in the model it is necessary to store the time after generation for each particle. The contribution of each particle to the total concentration of particles in a cell can then be found by multiplying its original contribution by a decay factor which depends on the time elapsed since generation β (where $\beta = \exp(-\lambda t)$ with λ = decay constant of tritium).

It appeared that results based on a time-dependent input of decaying particles were only reproducible after using a large number of particles. Even when the number of particles was increased to 20,000, the practical limit for the CDC®-*170/750* used, results were still not stable. For this reason several runs of each configuration were made and the derived concentrations were averaged. Averaging eight runs yielded stable results, while averaging five runs yielded workable results with less than 5% variation.

4. CALIBRATION OF THE MODEL

The calibration procedure of the mass-transport model can be split up into a calibration of the advective parameters and a calibration of the dispersive parameters. The advective parameters are: (1) configuration of large-scale heterogeneities (the clay lens at 18—20 m above m.s.l.); (2) permeability variations within the aquifer; and (3) effective porosity. The dispersive parameters are: (1) longitudinal dispersivity; and (2) transverse dispersivity.

The following discussion focuses on the variation of the separate parameters and their influence on calculated tritium profiles. Fig. 9A—E shows the results of numerous trials, where for each parameter the sensitivity is analysed with the others fixed on a best-fit value.

4.1. Clay-lens configuration

The position of the modelled piezometric (phreatic) surface is only influenced by aquifer transmissivity. This implies that differences in the clay-lens configurations, as sketched in Fig. 9A do not result in a significant variation of the modelled piezometric surface. It was, in fact, observed that a piezometric surface calculated with a simple formula (Ernst, 1973) for a homogeneous aquifer of constant thickness could fit all the modelled results for the phreatic surface.

However, the modelled tritium results reveal much about the necessity of dividing the aquifer into two subsystems separated by the clayey zone. It was also clear that the exact configuration of the clay lens does not significantly influence the tritium profile observed in boring V*1*.

4.2. Permeability

Fig. 9B shows the influence of variations in permeability on tritium transport. To prevent a smoothing of the tritium contrast in boring V*1* the permeabilities given in configuration *1* were chosen as optimal.

4.3. Porosity

An important factor in determining tritium concentrations and depth of tritium peaks is the ratio of net precipitation to effective porisity. Fig. 9C

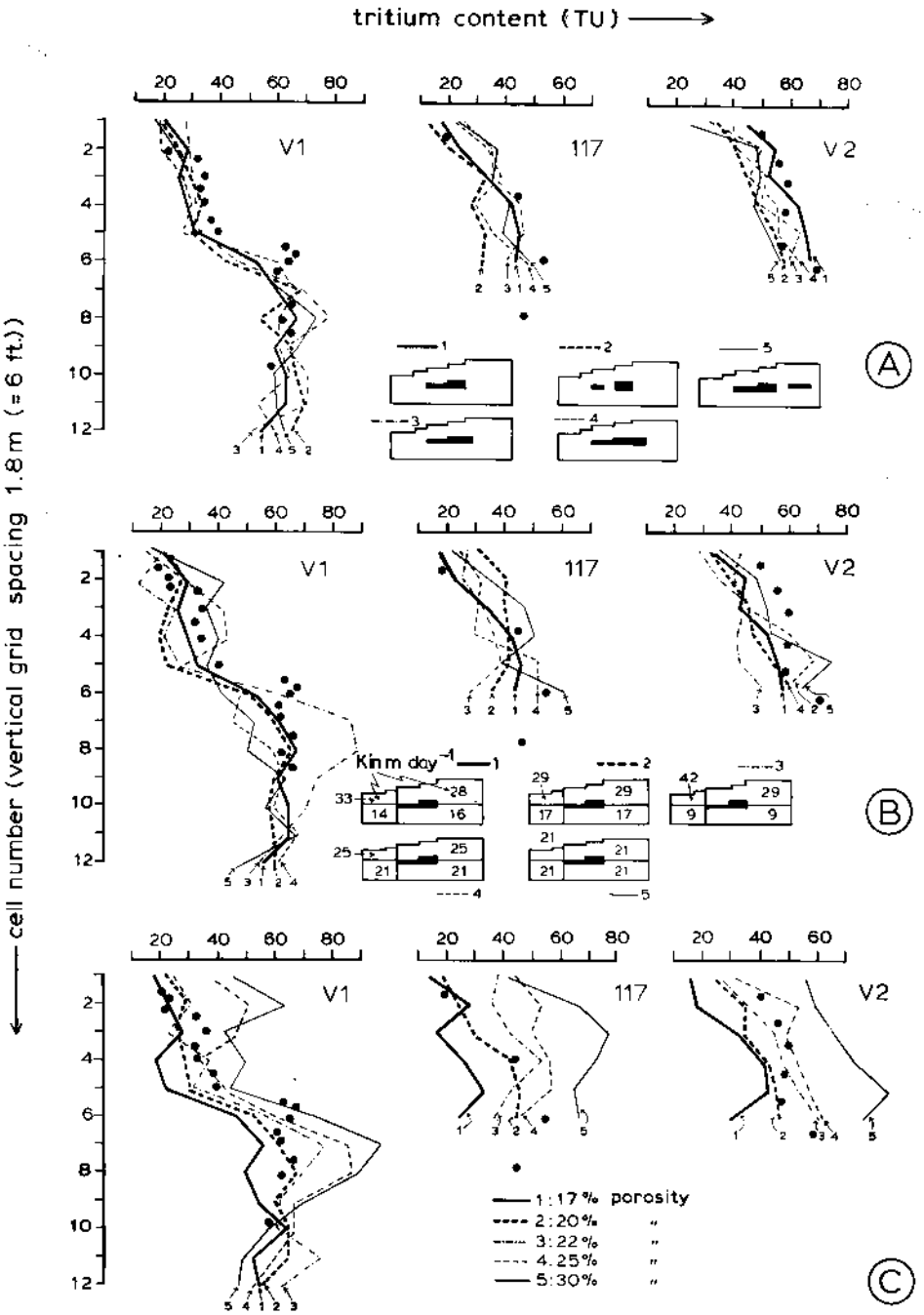
tritium content (TU) ⟶
20 40 60 80
20 40 60
20 40 60 80
V1
117
V2
2
4
6
8
10
12
3 1 4 5 2
2 3 1 4 5
5 2 3 4 1
1
2
3
4
5
A
Kin m day⁻¹
33
28
14
16
25
25
21
21
29
29
17
17
21
21
21
42
29
9
9
B
5 3 1 2 4
3 2 1 4 5
3 1 4 2 5
cell number (vertical grid spacing 1.8 m (= 6 ft.))
5 4 1 2 3
1 3 2 4 5
1 2 3 4 5
1 : 17 % porosity
2 : 20 % "
3 : 22 % "
4 : 25 % "
5 : 30 % "
C

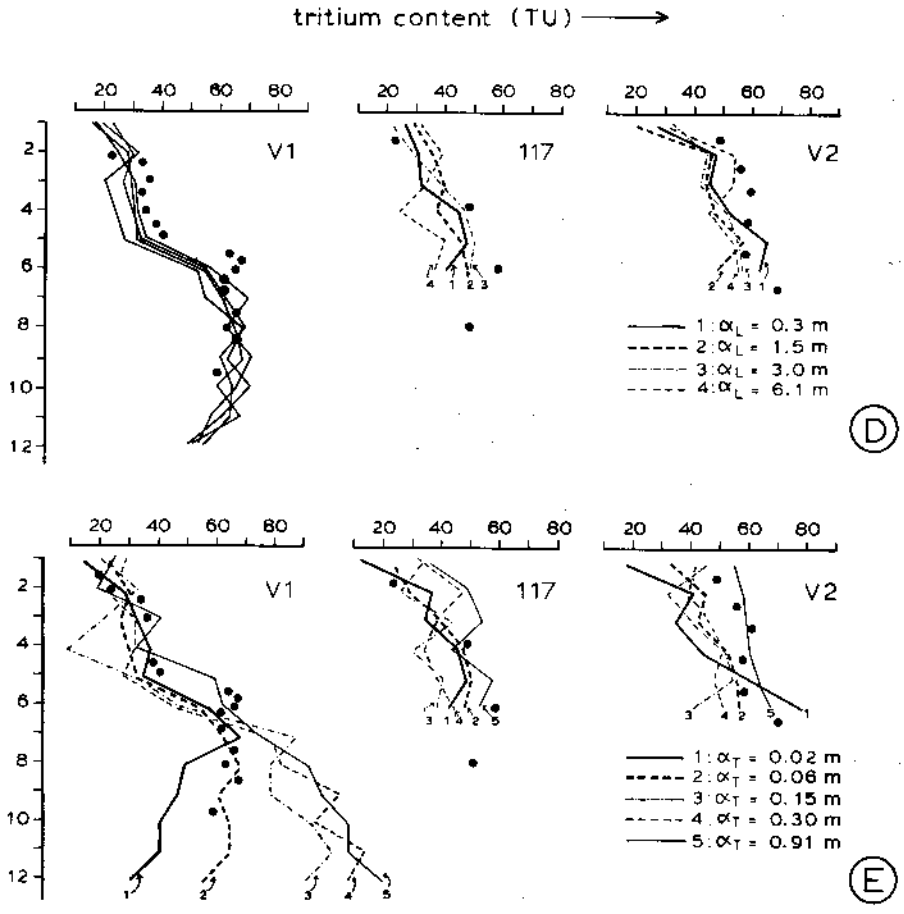

Fig. 9. Tritium profiles calculated for different aquifer conditions are compared with analysed values shown as *dots*. Sensitivity analysis is for: (A) configuration of large-scale heterogeneities; (B) permeability contrasts within the aquifer; (C) net precipitation over porosity; (D) longitudinal dispersivity; and (E) transverse dispersivity.

shows modelled results where effective porosity was varied within a reasonable range and net precipitation was fixed at 365 mm yr^{-1}.

It seems possible to distinguish different values for porosity within the aquifer, ranging from 20% to 25%. However, as the model was designed for a laterally uniform effective porosity, a compromise value (22%) is chosen.

4.4. Dispersivities

Longitudinal dispersivity was varied from 0.3 to 6 m. Fig. 9D shows that sensitivity for this parameter is absent. A good explanation for this phenomenon is that the tritium peaks occur as horizontal fronts in the

aquifer (this fact was checked with a special run simulating a one-peak input). Because of the nearly horizontal flow longitudinal dispersion moves the tritium particles only within these fronts of equal tritium content and thus has no influence on the final position of tritium peaks. In this respect it may be noted that the use of a dispersion formula developed for a point-source input as used by Egboka et al. (1983), cannot be valid in the situation where the input is uniform along the surface (as is the case with environmental tritium and a phreatic aquifer).

In logical contrast, the model is extremely sensitive to transverse dispersivity (α_T), which causes particles to move perpendicular to the streamlines. Because the amount of dispersive movement is proportional to the velocity, more particles will move from the shallow streamlines to the deeper streamlines than vice versa. Fig. 9E shows that when α_T is increased more particles flow under the clay lens and thus have a longer residence time in the model.

It should be kept in mind that although the chosen value of α_T is based upon the modelled concentrations in V*1* the value is mainly determined by flow around the upstream edge of the clay lens. Finally, we choose for α_L- and α_T-values of 3 and 0.06 m, respectively.

5. TRANSPORT OF WATER CONTAMINATED BY MANURE DEPOSITION

The calibrated model was used to simulate the transport of contamination originating from the heavily manured areas. Due to the complexity of nitrate hydrochemistry no absolute concentrations were modelled. Each time step (3 months) twenty "contaminating" particles were generated in the contaminated zone (Fig. 1) at the phreatic surface.

The computed pollution profiles (Fig. 10) show that the whole cross-section of the aquifer will be affected by pollution input on just a part of the surface. The calculations confirm that the loss of nitrate observed in the lower half of boring V*1* results from chemical reduction (denitrification) as previously postulated. From the observed vertical trends in concentration (Fig. 4), it appears that Cl^- concentrations closely match the calculated pollution profiles in borings *117* and V2, but not in V*1*. One would expect from the more constant Cl^- and SO_4^{2-} profiles observed in V*1* that water is almost completely vertically mixed at this point. However, the model calculations do show a dilution in the lower zone caused by water infiltrating in the upstream uncontaminated heath area.

The calculated profile of V*1*, in fact, most resembles that for the observed K^+ concentrations profile, although one should realize that K^+ concentrations are easily affected by adsorption.

The simulation of concentration levels after contamination stops shows a quick disappearance of the modelled conservative pollutant in borings *117* and V2 (i.e. without accounting for buffering reactions with soil and aquifer

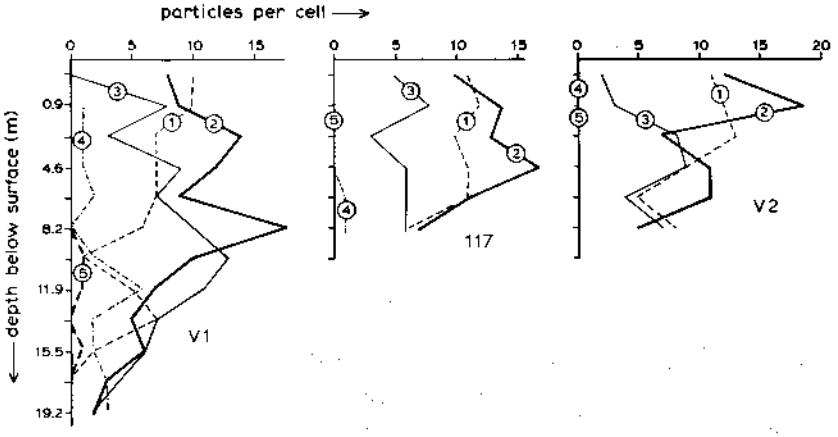

Fig. 10. Profiles showing a pollution history of 20 yr. A stationary input is applied in the first 8 yr., thereafter input stops, and aquifer flushing is followed during 12 yr. (*1*, *2*, *3*, *4* and *5* show situation after 4, 8, 12, 16 and 20 yr., respectively).

sediments). It is not surprising that the lower zone of boring V*1* holds its contamination much longer (>12 yr.). The quantitative effect of the clay layer which separates the aquifer into a quick and a stagnant system (Appelo et al., 1983) is nicely shown in this case.

6. CONCLUSIONS

The use of the Random Walk model for calculating mass transport in a cross-section and its calibration with tritium is a promising tool for the analysis of mass transport and hydrochemistry of a shallow phreatic aquifer. Tritium profiles obtained by detailed sampling of groundwater from boreholes at successive small depth intervals were used for model calibration. The following main points emerge from this calibration:

(1) The necessity of dividing the aquifer into two systems separated by the clay layer could easily be proven with the model. Attempts to specify the exact contours of the lens failed, but it could be proven that with the given degree of accuracy with which this "large-scale heterogeneity" was described also a reliable description of mass transport could be obtained.

(2) It was possible to optimize estimated permeabilities for four zones in which the aquifer was subdivided (based on geological assumptions in combination with knowledge about the total transmissivity).

(3) The model proved to be very sensitive to a variation in effective porosity (or rather: ratio of net precipitation to effective porosity). It should be questioned whether a more detailed description of porosity variations

should be included. At present the model does not offer the possibility to distinguish different porosities and field practice does not exist to enable the determination of porosity units.

(4) With tritium as a tracer in combination with horizontal groundwater flow, the model was only sensitive to transverse dispersivity (α_T). Moreover, the value for α_T resulted mainly from the flow situation at the upstream edge of the clay lens and therefore does not describe transverse mixing of flowlines elsewhere in the model. This dependency of the dispersion parameters on the scale and geometry of the model (already mentioned in the literature, e.g., Fried, 1981) makes the usefulness of these parameters rather questionable.

The promising results obtained by tritium calibration of model parameters like the clay-lens extension, permeability variations and porosity suggests that the dispersive part of the description of mass transport could be reduced to its original function, namely, to simulate the diffuse mixing between adjacent flowlines due to a grained porous medium.

The main point is, of course, how the necessary subsoil hydraulic information can be obtained without a very detailed boring and permeability measurement program.

It seems hardly possible to obtain information on small-scale geologic perturbations, which would be necessary for a true deterministic physical model. Using tritium, which presents a water-quality record of the last 30 years, as a calibration parameter for the mass-transport model, one is able to provide a tool which allows the calibration of geologically based assumptions relating to spatial permeability and porosity distribution. Methods such as proposed by Smith and Schwartz (1981) and Smith (1981) to relate the variation of sedimentary properties to the variation of the hydraulic properties of the flow domain can be tested with calibration procedures described above.

ACKNOWLEDGEMENTS

The authors wish to thank Professors N.A. de Ridder and I. Simmers for their help in establishing a good text written in proper English and Professor A. van der Beken (Hydrological Service, Free University Brussels) for providing optimal computational facilities.

REFERENCES

Appelo, C.A.J., Krajenbrink, G.J.W., Van Ree, C.C.D.F. and Vasak, L., 1983. Influences on groundwater quality in the northwestern Veluwe, The Netherlands. Min. Environ. Prot., The Hague, Ser. Soil Prot. 11, 140 pp. (in Dutch).

Bear, J., 1972. Dynamics of Fluids in Porous Media. American Elsevier, New York, N.Y., 764 pp.

Boonstra, J. and De Ridder, N.A., 1981. Numerical modelling of groundwater basins. Inst. Land Reclam. Improve. (I.L.R.I.), Wageningen, Publ. 29.

Carlston, C.W., Thatcher, L.L. and Rhodehamel, E.C., 1960. Tritium as a hydrologic tool — The Wharton Tract study. Int. Assoc. Sci. Hydrol., Publ. No. 52, pp. 503—512.

Crommelin, R.D. and Maarleveld, C.G., 1952. Fluvioglacial clay in the northern Veluwe. Boor Spade, 5: 118—125 (in Dutch).

Egboka, B.C.E., Cherry, J.A., Farvolden, R.N. and Frind, E.O., 1983. Migration of contaminants in groundwater at a landfill: a case study, 3. Tritium as an indicator of dispersion and recharge. J. Hydrol., 63: 51—80.

Ernst, L.F., 1973. The determination of transport time of groundwater during flow in the saturated zone. Inst. Land Water Manage. Res. (I.C.W.), Wageningen, Nota 755 (in Dutch).

Fried, J.J., 1981. Groundwater pollution mathematical modelling: improvement or stagnation? Sci. Total Environ., 21: 283—298.

Kovács, G., 1981. Seepage Hydraulics. Elsevier, Amsterdam, 730 pp.

Meinardi, C., 1974. Chemical composition of groundwater of the Veluwe. Inst. Drinking Water Supply (R.I.D.), Voorburg, Med. 1974-4 (in Dutch).

Prickett, T.A., Naymik, T.G. and Lonnquist, C.G., 1981. A "random walk" solute transport model for selected groundwater quality evaluations. Illinois State Water Surv., Champaign, Ill., Bull. 65.

Smith, L.W., 1981. Spatial variability of flow parameters in a stratified sand. Math. Geol., 13: 1—21.

Smith, L.W. and Schwartz, F.W., 1981. Mass transport, 2. Analysis of uncertainty in prediction. Water Resour. Res., 17: 351—369.

Vasak, L., Krajenbrink, G.J.W. and Appelo, C.A.J., 1981. The spatial distribution of polluted groundwater from rural centres in a recharge area in The Netherlands — The Veluwe. Sci. Total Environ., 21: 105—112.